Journal of Solid and Fluid Mechanics (JSFM)

Shahrood University of Technology

Manufacturing Engineering of Iran

Experimental and numerical investigation of thickness distribution, drawing depth, and forming limit diagram of steel sheet using Nakazima test

Seyed Hamid Seyed Salehi[1], Farnoosh Turki[2], Abdolhossein Jalali Aghchei[3], Mohammad Javad Bakhtiary Doost[4]

[1]M.S.c, K.N. Toosi University of Technology
[2]Ph.D Student, K.N. Toosi University of Technology
[3]Associate Professor, K.N. Toosi University of Technology
[4]M.S.c, K.N. Toosi University of Technology
*Corresponding author: jalali@kntu.ac.ir

Abstract

In this article, the mechanical properties of stainless steel are measured at different strain rates. Then, considering the Swift work-hardness equation, the forming limit diagram (FLD) of the sheet has been obtained with two experimental and finite element methods. After designing the experiment based on the Box-Behnken method and performing them using the finite element method, the effect of different parameters on the depth of the product without tearing has been obtained. Finally, the optimal parameters to achieve the maximum stretching depth have been extracted. After defining the properties extracted from the steel sheet in the software, in order to validate and ensure the accuracy of the finite element analysis, the thickness distribution in a certain path on the experimental product has been compared with the finite element. After designing the experiments and conducting them using the FEM, it was found that in the investigated range, the clearance between the punch and the die has no effect on the depth of tension; Also, by increasing the radius of the opening of the die, the depth of stretching increases. The coefficient of friction has the greatest effect on the depth of stretching and with its decrease, the depth of stretching increases.

1. Introduction

Deep drawing is a highly efficient and widely used manufacturing process in the field of sheet metal forming. It involves the transformation of a flat sheet metal blank into a three-dimensional shape, typically a cup or a cylindrical component, by applying significant forces and pressure. This process is commonly employed in various industries, including automotive, aerospace, appliance manufacturing, and many others [1]. Deep drawing relies on the principle of plastic deformation, where the metal sheet is subjected to intense stretching and bending forces, causing it to flow into a die cavity and take the shape of the desired product. The process is usually performed using specialized machinery called deep drawing presses, which exert precise control over the applied forces and movement [2]. The success of deep drawing depends on several key factors, such as the material properties of the sheet metal, the geometry of the die and punch, lubrication, and the applied forces. The choice of material is crucial, as it must possess sufficient ductility to withstand the deformation without cracking or tearing. Commonly used materials for deep drawing include aluminum, stainless steel, and mild steel [3]. The design of the die and punch is another critical aspect of the deep drawing process. The die cavity must be carefully designed to accommodate the desired shape and ensure a smooth flow of the material. The punch applies the necessary forces to deform the sheet metal and push it into the die cavity. Lubrication is essential to reduce friction and prevent the sheet metal from sticking to the die or punch.

Deep drawing offers several advantages in manufacturing. It allows for the production of

complex shapes with high precision and repeatability. The process is also highly efficient, as it enables the production of multiple components from a single sheet of material, reducing material waste. Additionally, deep-drawn components often exhibit excellent structural integrity and strength [4].

The Forming Limit Diagram (FLD) is a crucial tool used in the field of sheet metal forming to assess the formability and predict the occurrence of necking and fracture during the manufacturing process [5-8]. It provides valuable information about the maximum strains that a sheet metal material can sustain without failure under different deformation conditions. The FLD helps engineers and manufacturers optimize their forming processes, select appropriate materials, and avoid costly defects [9,10]. Keeler and Backofen's in 1963 work on plastic instability and fracture in sheets stretched over rigid punches is referenced to emphasize the early development of FLDs [11]. A study also confirms advances in computational forming mechanics, in the analysis, modeling and optimization of metal forming. This highlights the integration of numerical simulations and FLDs to predict formation limits and optimize process parameters [12].

According to the mentioned great importance of checking sheet formability curves in the industry, achieving the best forming limit has a special place. In addition to the mentioned cases, checking the sheet thickness distribution and validating the results with the experimental model are among the tasks that were used for the design of the die. The analysis of isotropic coefficients and coefficients of Swift's equation is also done in this article. Finally, using the results of the mechanical properties of materials in the finite element method led to the agreement of the obtained results.

2. Methodology

2.1. The experimental procedure

The material used in this article is a 304 stainless steel sheet with a thickness of 0.8 mm. To determine the mechanical properties of the target sheet, two main tests were employed: uniaxial tensile tests and Nakazima test (expansion with a spherical punch). Tensile tests are performed at three speeds: 5.2 mm/min, 12.6 mm/min, and 250 mm/min. Each speed is repeated twice. In the experiments, 6 samples were taken in the direction of zero degree to check the effect of strain rate and 3 samples were taken to check the effect of anisotropy (one sample at a 45-degree angle and one sample at a 90-degree angle to the rolling direction). Figure 1. shows the stretch forming die.
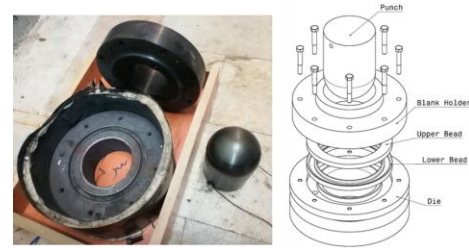

Figure 1. Stretch forming die used in experimental test

2.2. Design of experiment based on RSM method

The objective of this article is to optimize the input parameters to reach the maximum depth of draw until the first element of the sheet enters the 10% strain region of the Forming Limit Diagram (FLD) curve or to achieve a reduction in sheet thickness within the 50% range of the initial thickness.

The Box-Behnken design method based on the Response Surface Methodology (RSM) was utilized in this article for optimizing the parameters. In this case, considering that the dimensions of the product are predetermined and cannot be changed, the variables that can be considered as inputs include the coefficient of friction (COF), blank holder force, die entry radius, sheet rolling direction, and clearance between the punch and die. Table 1 displays the parameters under investigation and the levels of each parameter.

Table 1. The selected parameters and levels for experimental design

Symbols	Parameters	Levels	Unit
A	Clearance	1.75-2.5	mm
B	Die Radiuses	3.2-6.4	mm
C	COF	0.1-0.2	-
D	Blank holder force	60-138	KN
E	Roll direction	0-45	Degree

2.3. The finite element method (FEM) process

The components of the considered dies, including the punch, die, and blank holder, are modeled as interdependent and parametric entities in CATIA software. The dimensions considered for the blank holder, punch, and die are shown in Figure 2. The parameterized values specified in the figure are presented in Table 2.
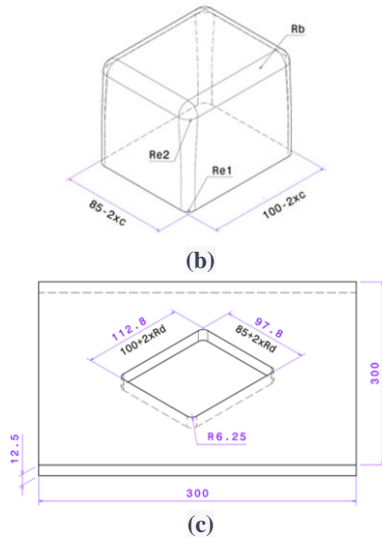

(a)

(b)

(c)
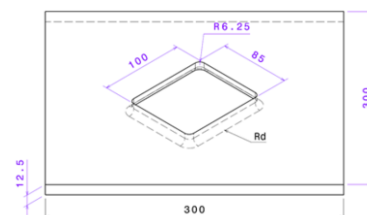
Figure 2. The dimensions of (a) the die, (b) the punch, and (c) the blank holder

Table 2. Geometric specifications of the used dies

R_{e2} (mm)	R_{e2} (mm)	R_b (mm)	R_d (mm)	C (mm)
			3.2	0.8
6.25	8.75	8.75	4.8	1.4
			6.4	2

Each element within the mesh has a maximum chord size of 10 mm. The sheet thickness is assumed to be 0.8 mm, and the material properties are selected based on the predefined properties of the steel sheet within the software. In the process section of the PL branch, the friction conditions between all corresponding components are defined, and the desired value for the Coulomb friction coefficient is specified. The punch and die are treated as rigid bodies, while the sheet holder is modeled as an elastic body. Within the simulation section, specifically in the control branch, there is flexibility to modify parameters associated with sheet meshing. Shell-type elements with 11 integral points along the thickness (EPS-11) are utilized, and the problem is treated as plane stress. Figure 3. depicts the meshing and assembly of the mold components.
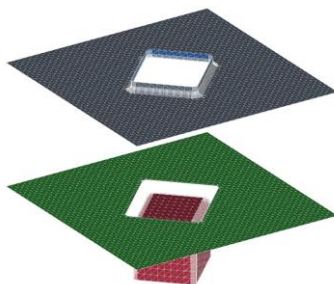

Figure 3. Meshing and assembly of mold components

In Figure 3, the blank holder is highlighted in green, the punch is shown in red, and the die is indicated in blue.

3. Discussion and Results

3.1. elastic property

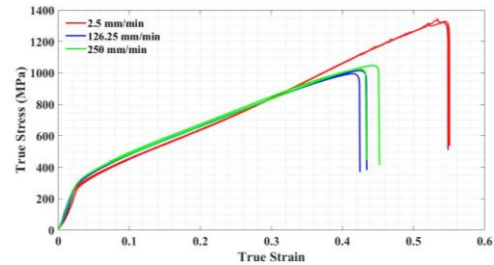Figure 4. shows true stress versus true strain curve.

Figure 4. Curves related to tensile test at different speeds

It is expected that with an increase in strain rate, the required force for forming will also increase. Since a higher speed of the jaws' movement results in a higher rate of work done on the material, the heat generation rate in the material increases. However, due to convective heat transfer between the specimen and the air, this generated heat is not adequately exchanged with the surroundings. As a result, the temperature of the specimen increases during the test. As the temperature increases, the yield stress of the steel decreases. Therefore, the curves corresponding to higher speeds intersect with the curve corresponding to a speed of 2.5 mm/min. Additionally, due to the low thickness of the specimen and the high yield stress of stainless steel 304, a reduction in the width of the specimen was observed in the region held by the jaws, both before and after the test, by approximately 1 mm. This indicates that material flow occurred not only in the gauge area but also in the jaw region during the test. Figure 5. illustrates the material flow in the jaw region during the test.

Figure 5. Flowing of material from the jaw during the test

When fitting the curve in MATLAB, data points corresponding to strains higher than 0.2 were excluded from the analysis. A power-law curve has been fitted to this graph, which represents the

coefficients in the strain-hardening relationship, specifically the Swift exponent.

By fitting the data, the constant values of the shear equation are obtained, which is in accordance with Equation 1.

$$\sigma = c * (\varepsilon_{pl} + \varepsilon_0)^m \qquad (1)$$

In the Swift work hardening equation (equation 1), c and m are material constants. ε_0, in fact, represents the strain at which the material reaches its yield point. It is commonly referred to as the yield strain and ε_{pl} represents the plastic strain. displays the coefficients c and m obtained from fitting the curve to the data on the graphs (Table 3.).

Table 3. Coefficients obtained from curve fitting on graphs

m	C	Jaw movement speed (mm/min)	Number of experiments
0.4405	1287	2.5	1
0.4560	1316	2.5	2
0.4168	1269	126.25	3
0.4274	1295	126.25	4
0.4274	1305	250	5

The value of $\overline{R}$ is 0.1 for the case where thickness is measured in micrometers, and it is 1.1 for the case where theoretical calculations are performed. The theoretical results have been utilized in the finite element analysis.

3.2. finite element method validation with experimental result

The thickness distribution in an industrial product subjected to deep drawing process is examined as an output parameter between the finite element analysis and the experimental data. Figure 6. illustrate the comparison between two methods.
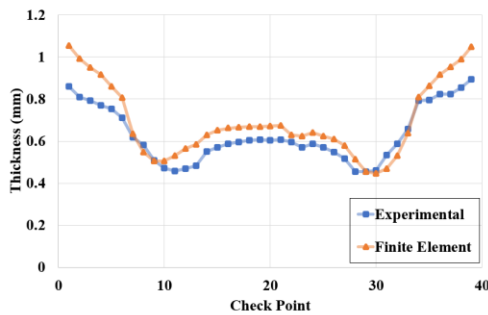

Figure 6. The graph compares the thickness between the finite element analysis and experimental measurements.

According to the comparison conducted in Figure 6, the average relative measurement error between finite element analysis and experimental data was calculated to be 8.11%.

In order to find the optimal parameters, the optimization section in the Minitab software has been used by analyzing the results. The maximum response value occurs for the minimum value of the sheet clamping force within the tested range, the maximum value of the matrix radius, and the minimum value of the friction force. After optimizing the parameters, simulations were performed again to verify the accuracy of the proposed values for the optimal condition. As observed, the predicted value for the response closely matches the obtained response value from the simulation, indicating a high level of accuracy (Figure 7).
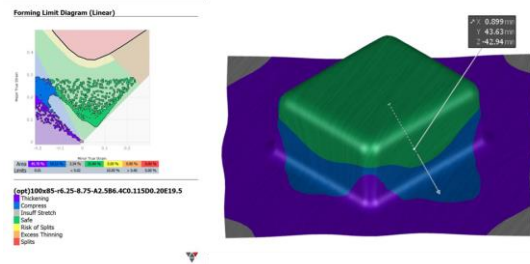

Figure 7. Finite element analysis with optimal parameters

As observed in Figure 7., the tension depth prior to entering the excessively thinning region is obtained as 94.42 millimeters, which differs by 1% from the predicted value.

4. Conclusion

In this paper, the finite element analysis of the deep drawing process of a rectangular cup with a stainless steel 304 sheet was performed to investigate the influential parameters on the depth of draw. By extracting the formability properties of the steel sheet, the effect of various parameters on the depth of draw was examined. After designing the experiments using the Box-Behnken method and conducting them using the finite element method, it was determined that the clearance between the punch and the die has little effect on the depth of draw. Moreover, an increase in the die corner radius results in an increase in the depth of draw. The friction coefficient has the most significant effect on the depth of draw, and a decrease in the friction coefficient generally leads to an increase in the depth of draw. Decreasing the blank holder force also increases the depth of draw, while changing the rolling direction does not significantly affect the depth of draw.

Thus, the depth of draw is directly related to the die corner radius and inversely related to the friction coefficient and blank holder force. Finally, by utilizing the response surface methodology, the optimal parameters for achieving the maximum depth of draw without causing tearing were obtained.

5. References

[1] Tebbe, P. A., & Kridli, G. T. (2004). Warm forming of aluminium alloys: an overview and future directions. *International Journal of Materials and Product Technology*, *21*(1-3), 24-40.

[2] Ghennai, W., Boussaid, O., Bendjama, H., Haddag, B., & Nouari, M. (2019). Experimental and numerical study of DC04 sheet metal behaviour—plastic anisotropy identification and application to deep drawing. *The International Journal of Advanced Manufacturing Technology*, 100, 361-371.

[3] Singh, C. P., & Agnihotri, G. (2015). Study of deep drawing process parameters: a review. *International Journal of Scientific and Research Publications*, 5(2), 1-15.

[4] Swapna, D., Ch, S. R., & Radhika, S. (2018). A review on deep drawing process. *International Journal of Emerging Research in Management and Technology*, 6(6), 146-149.

[5] Keeler, S. P. (1961). Plastic instability and fracture in sheets stretched over rigid punches (Doctoral dissertation, *Massachusetts Institute of Technology*.

[6] Bleck, W., Deng, Z., Papamantellos, K., & Gusek, C. O. (1998). A comparative study of the forming-limit diagram models for sheet steels. *Journal of Materials Processing Technology*, 83(1-3), 223-230.

[7] Ozturk, Fahrettin, and Daeyong Lee. "Analysis of forming limits using ductile fracture criteria. *Journal of Materials Processing Technology 147*, no. 3 (2004): 397-404.

[8] Obermeyer, E. J., & Majlessi, S. (1998). A review of recent advances in the application of blank-holder force towards improving the forming limits of sheet metal parts. *Journal of Materials Processing Technology*, 75(1-3), 222-234.

[9] Fourment, L., & Chenot, J. L. (1996). Optimal design for non-steady-state metal forming processes—I. Shape optimization method. *International journal for numerical methods in engineering*, 39(1), 33-50.

[10] Graf, A. F., & Hosford, W. F. (1993). Calculations of forming limit diagrams for changing strain paths. *Metallurgical and Materials Transactions A*, 24(11), 2497-2501.

[11] Keeler, S. P. (1961). Plastic instability and fracture in sheets stretched over rigid punches (Doctoral dissertation), Massachusetts Institute of Technology.

[12] Davim, J. P. (Ed.). (2012). Computational Methods for Optimizing Manufacturing Technology: *Models and Techniques: Models and Techniques. IGI Global*.